ARPA-E Quarterly Technical Report
Award - DE-AR0001559
Quarter 6 (November 1, 2023 – January 31, 2024)

Project Title: Quantifying the Potential and Risks of Large-Scale Macrophyte Cultivation and Purposeful Sequestration as a Viable CO2 Reduction (CDR) Strategy (SeaweedCDR)

This is the sixth quarterly report for the SeaweedCDR project, covering the period November 1, 2023 to January 31, 2024. As you may recall, we had an issue in completing M2.1 (Design & Implement Seaweed Packaging) as planned due to the lack of large quantities of giant kelp biomass available for purchase. We agreed to push back this deliverable, as well as the next two deliverables, M2.2 (Seaweed Biomass Fates Methods Development - a go/no go milestone), and M2.3 (Validation of Biomass Fate Methods) a quarter. Task M2.3 is now this quarters deliverable. The goal for task M2.3 is to validate the methods to assess the fate of kelp biomass through a series of laboratory and field-based experiments that were outlined in the previous quarter and in a recently uploaded white paper (Krause et al., 2023). Considerable progress has been made in laboratory-based experiments, however, due to unforeseen complications, progress in the field experiments have been slowed, which will be discussed further in this QR. We will need another quarter of extension to get this work accomplished.

Other deliverables are M4.4 (Model development and system documentation) and M6.3 (First iteration of the T2M plan). Both are complete with the model documentation white paper nearly ready for submission to the preprint server. We have also made progress on M6.7 (Scientific Outreach) to report on.

Task 2 – Quantification of Seaweed Biomass Fates

Deliverable: M2.3 – Validation of biomass fates methods - Completion level – 50%

Leads: Sebastian Krause, Bob Miller & David Valentine (UCSB)

The goal for task M2.3 is to validate the methods to assess the fate of kelp biomass through a series of laboratory and field-based experiments that were outlined in the previous quarter and in a recently uploaded white paper (Krause et al., 2023). This deliverable had been previously extended by 1 quarter. Considerable progress has been made in laboratory-based experiments, however, due to unforeseen complications, progress in the field experiments have been temporarily slowed, which will be discussed further in this QR.

Laboratory Sinking Rate Experiments

In the laboratory, we performed sinking rate experiments with Giant kelp biomass, which is outlined in detail in a white paper uploaded to Earth ArXiv (Krause et al., 2023). Briefly, in the lab, kelp fronds were dissected into components (i.e., stipe, blades and pneumatocysts) and

weighed wet. To determine the sinking rates of masticated kelp biomass the dissected kelp components were dropped into a vertical cylinder filled with seawater and the sinking of the kelp components were filmed with a camera. Sinking rates were calculated by dividing the distance traveled by the video recording time. Figure 1 shows the results of the sinking rate experiments.

Generally, stipe fragments had the highest sinking rates over the other kelp components (Max sinking rate; 0.25 m s^{-1}), while blades and pneumatocysts had similar sinking rates (Max sinking rates; 0.08 and 0.1 m s^{-1}, respectively) (Fig. 1). On average sinking rates were 0.087 m s^{-1} ± 0.531 (n = 28) for stipes, 0.033 m s^{-1} ± 0.028 (n= 30) for blades and 0.053 m s^{-1} ± 0.22 (n = 20) for the pneumatocysts. The results from these experiments show large variation in the sinking rates of the kelp components. We calculated the precision in our experiments by taking the percent quotient of the standard deviation and the mean. The precision in our experiments showed a 53%, 84%, and 41% spread from the average sinking rates of stipes, blades, and pneumatocysts, respectively. However, our sinking rate data is similar to the sinking rates of macroalgal fragments from a different macroalgal species *Laminaria hyperborean*. Wernberg and Filbee-Dexter, (2018) conducted sinking rate experiments within a marina and reported sinking rates of *L. hyerborean* blade fragments ranging in wet weight between 0.034-82.2 g and determined the blade fragment sinking rates were between 0.022 m s^{-1} and Max 0.15 m s^{-1}. Their study also reported sinking rates for stipe fragments weighing between 334-526 g to be between 0.1 and 0.333 m s^{-1}. Although our sinking rate data show larger variability than expected for this SOPO, our data also suggests that masticated Giant Kelp detrital biomass does sink fast, on the order of 1000's of meters per day. We will be using these data to estimate the sinking rates of whole Giant kelp fronds, which will give us expectations for future field measurements.

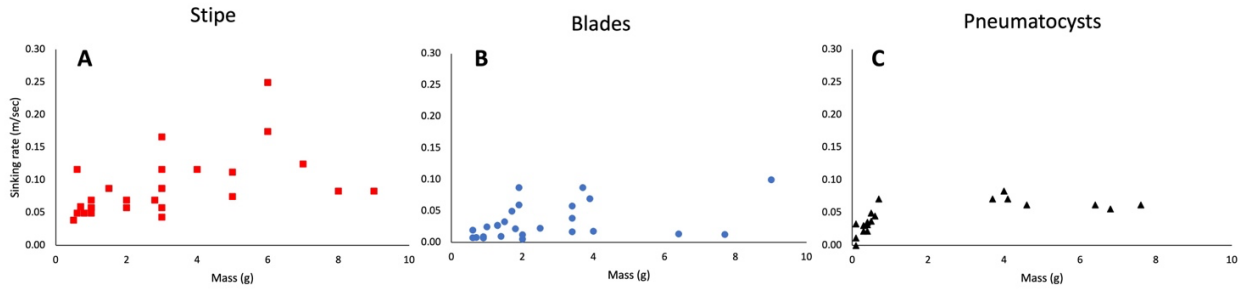

Figure 1. Results from laboratory based sinking rate experiments using Giant kelp components stipe (A), blades (B) and pneumatocysts (C)

Laboratory based kelp degradation incubations

For laboratory based kelp degradation incubations, we followed the procedures outline in Krause, (2023). We have conducted two incubations: The first incubation used anoxic seawater from approximately 585 meters within the Santa Barbara Basin, during a research cruise on *R/V Atlantis.* The second incubation used oxygen rich seawater from the UCSB Marine Science Institute. Briefly, Giant kelp was dissected into kelp components similar to the above section. We also included a set of bags with more intact segments of the Giant kelp frond to represent

less masticated kelp (Whole) (Fig. 2D). Approximately 50 grams (wet weight) of kelp components were added to polynylon plastic heat seal bags, equipped with a custom-made sampling port (Fig. 2). Seawater was then added into the bags either through the sampling port of a sealed bag or prior to heat sealing. The bags containing kelp biomass and seawater were kept in the dark and at 4°C to mimic the placement of Giant Kelp at the seafloor. Seawater within the bags was periodically sampled for particulate organic carbon (POC), dissolved organic carbon (DOC), and dissolved inorganic carbon (DIC). Note the duration of the incubations differed between the anoxic and oxic incubations. The anoxic incubations lasted for 1 to 2 weeks and the oxic incubations lasted for 2 weeks.

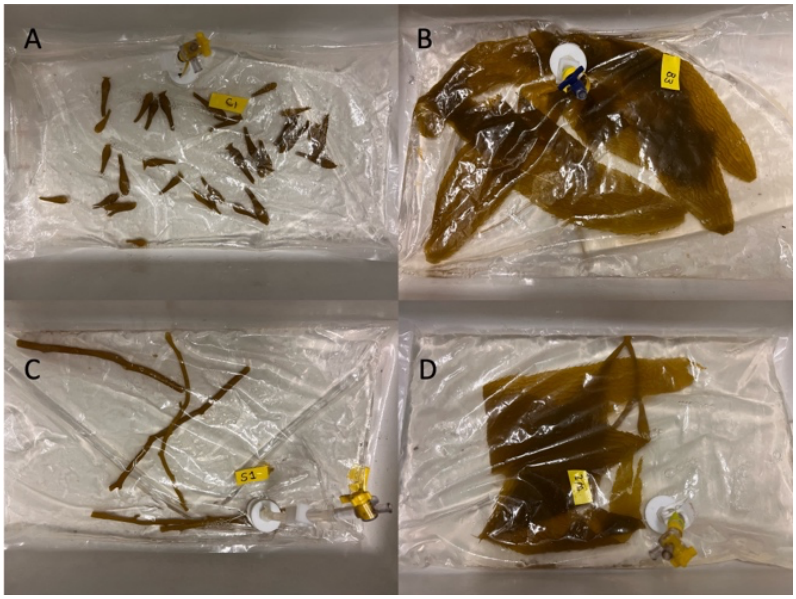

Figure 2. Photos of poly nylon bags containing Giant Kelp biomass components; pneumatocyst (A), blades (B), stipes (C), and whole intact segment (D).

Changes in Particulate Organic Carbon (POC) during incubations

For our purposes we are categorizing the POC from Giant Kelp as having two pools, large and small POC (LPOC and SPOC, respectively). The LPOC is the leftover bulk kelp biomass left inside the bag that could not fit through our custom sampling port (8.5 mm), while the SPOC fraction is the organic carbon that fits through the sample port and is captured onto filters with a 0.3 µm pore size. Please note that data for LPOC is currently being analyzed and is not included in this document; however, we anticipate that the data will be available to discuss in the QR meeting in March. Figure 3 shows the results of the SPOC from both anoxic and oxic kelp degradation incubations. The results show that less SPOC was produced during the anoxic incubations than during the oxic incubations. Blades in the anoxic incubations produced the most SPOC while stipe biomass produced more SPOC than the rest of the components during the oxic experiments.

During the anoxic incubations, average SPOC started (T0) lower across all bags with kelp components ranging between 5.8 and 142 µmols C L^{-1} and then after 353 hours (TF) the SPOC increased between 15 and 723 µmols C L^{-1} (Fig. 3A). The precision of the method was calculated by taking the percent quotient of the standard deviation and the average. The precision for the T0 samples ranged between 3.5% and 26% and between 3% and 94% at TF.

For the oxic incubations, average SPOC values at T0 for the seawater control were low at 3.8 µmols C L^{-1} (Fig. 3B). T0 SPOC for the sample bags with stipes, blades and whole segments ranged between 25 and 27 µmols C L^{-1}. While bags with pneumatocysts started with SPOC at 155 µmols C L^{-1}. SPOC in the middle of the incubation (TM) increased by 1 to 2 orders of magnitude. TM SPOC average concentrations were 98, 436, 600, and 701 µmols C L^{-1} for bags with pneumatocysts, stipes, blades, and whole segments, respectively. At TF, SPOC increased again by 1 to 2 orders of magnitude to 686, 2912, 1351, and 1237 µmols C L^{-1} for bags with pneumatocysts, stipes, blades, and whole segments, respectively. In most cases the precision of the SPOC analysis from the oxic incubations could be determined within 10% of the average as stated by the SOPO, however, in a few instances the spread of the data did exceed the 10% threshold reaching as high as 54%.

We believe that some of the large variation specifically for the anoxic incubations may be explained by the challenges of measuring accurate weights on moving research vessels. But is also partly due to unforeseen challenges in collecting the SPOC samples. To estimate the degradation products that are not captured in the DOC fraction (0.2um and smaller), we filtered seawater for POC using a 0.3um pore size. POC determinations in open ocean settings often requires large quantities of filtered seawater (2L) to obtain detectable amounts of POC on the filter. Initially, we did not know how much water from our incubations needed to be filtered to get detectable amounts of POC. We found through our experiments that there is sufficient POC on the filter given smaller volumes of kelp seawater (i.e., 100-500 mL). In addition, towards the end of the incubations, we noticed there was more “slime” that we speculate is coming from the kelp, which quickly clogs the 0.3 µm filter, meaning there could be more pools of POC at different size fractions. Moving forward we will plan to repeat our incubations and optimize our methods to filter water through multiple filters with variable pore sizes to not only expedite the sample collection but to identify other POC pools that are derived from the kelp.

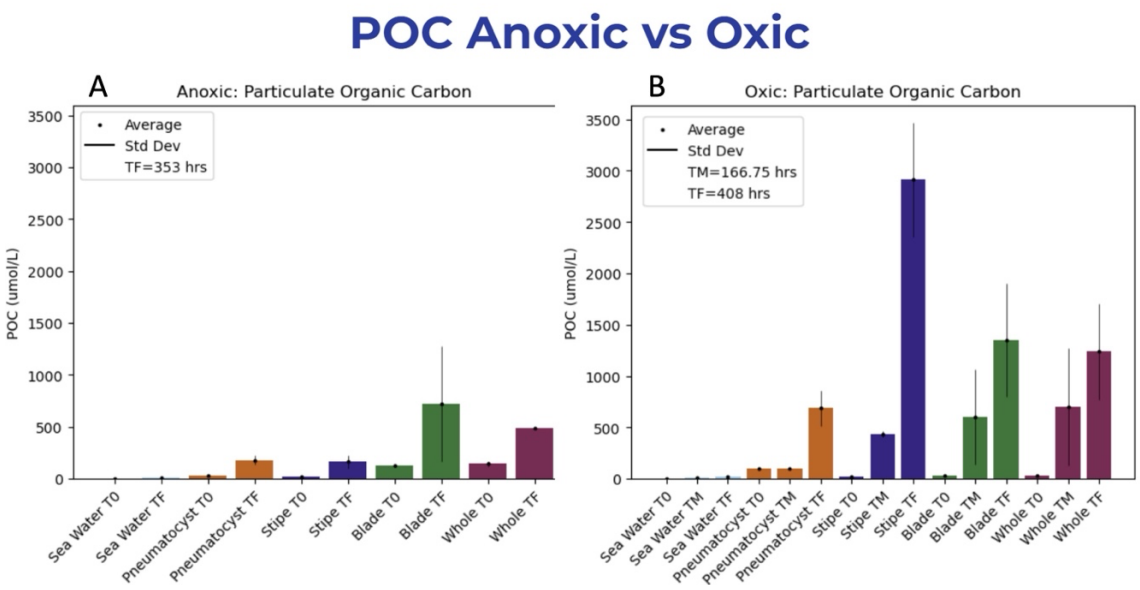

Figure 3. Results from POC analysis from Giant Kelp components during the anoxic (A) and oxic (B) incubations.

Changes in Dissolved Organic Carbon (DOC) during incubations

Samples for DOC were also collected in both the anoxic and oxic kelp degradation incubations. Generally, in the anoxic incubations we saw an order of magnitude difference in the DOC released in the bags with blades and whole intact segments (Max average 24,536 ± 17,959 µM for blades; 43,944 ± 21,812 µM for whole) than with the pneumatocysts and stipe (Max average 5,322 ± 4,333 µM for pneumatocysts; 6,414 ± 4,720 µM for stipes) over the course of 150 hours (Fig. 4B-E). We calculated the precision of the methods by taking the % quotient of the standard deviation and the average value for each treatment. We found large variation that do exceed the 10% threshold in our SOPO (pneumatocysts 18-81%; stipe 17-74%; blades 57-76%; whole 43-134%). We believe some of this variation is natural (i.e., variation across technical replicates to which the average is calculated). However, the variation is also likely due to the challenges of weighing and measuring kelp biomass and seawater volumes on a moving vessel. Nevertheless, we applied what we have learned in the anoxic incubations to our oxic incubations which were done in a more controlled setting at UCSB.

Interestingly, compared with the anoxic incubations, the DOC buildup was delayed during the oxic incubations (Fig. 4F-J). The bags with blades and whole intact segments during the oxic incubation released more DOC after 150 hours (Max average 1,745 ± 2,078 µM for blades; 1,270 ± 1,045 µM for whole) compared to the bags with pneumatocysts and stipes (Max average 97 ± 15 µM for pneumatocysts; 439 ± 120 µM for stipes) (Fig. 4G-J). Please note that DOC samples for the two-week timepoint are currently being analyzed and will be discussed in the QR meeting in March. The precision of the method in this case was slightly better than the previous anoxic incubation. However, we do still see large variations that do exceed the 10% threshold in our SOPO (pneumatocysts 7-29%; stipe 3.5-27%; blades 6-119%; whole 27-108%). In this

instance we believe that the majority of the variation is due to natural causes (i.e., different batch of kelp, kelp health, and variation amongst the technical replicates that the average is calculated).

We used this information to calculate preliminary DOC release rates for anoxic and oxic incubations. In the anoxic incubations we found the blades had the highest release rate (39.1 µmolC g_{dw} hr^{-1}) compared to the pneumatocysts and stipe DOC release rates (8.5 and 9.3 µmolC g_{dw} hr^{-1}, respectively). The sum of all these release rates (56.9 µmolC g_{dw} hr^{-1}) do closely resemble the DOC release rate of the whole intact segment (57.3 µmolC g_{dw} hr^{-1}). In the oxic incubations, blades had the highest DOC release rate but was lower than the anoxic incubations (8.3 µmolC g_{dw} hr^{-1}). The DOC release rate of the pneumatocysts and stipes were lower than the blades (0.2 and 1.9 µmolC g_{dw} hr^{-1}, respectively) but within similar ranges reported by (Reed et al., 2015; English and Carlson, 2023). Our preliminary interpretation of these patterns is that presence of oxygen helped keep the kelp biomass alive, thus inhibiting/ delaying the DOC release from senescence. Whereas the lack of oxygen in the anoxic incubations may have stressed the kelp biomass, thus releasing more DOC earlier.

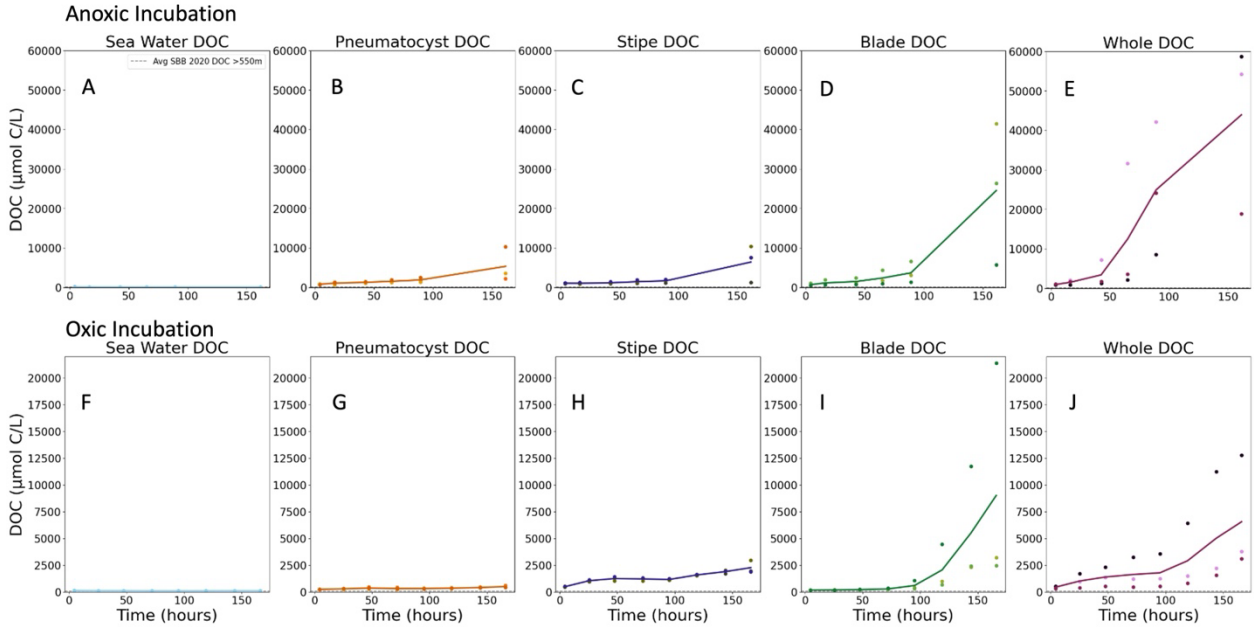

Figure 4. Results showing the evolution of DOC concentrations in bags containing Giant Kelp components during the anoxic (A-E) and oxic (F-J) kelp degradation incubations.

Changes in Dissolved Inorganic Carbon (DIC) during incubations

Samples for DIC were also collected in both the anoxic and oxic kelp degradation incubations. In the anoxic incubations, DIC in all bags with kelp component biomass appeared to have a slight decrease after approximately 89 hours, before slightly increasing again after 161 hours (Fig. 5A-E). Bags with blades and whole intact segments had more DIC at the end of the anoxic incubation (Max average DIC concentrations 2,479 µM ± 287 and 2,270 µM ± 510, respectively) than the bags with pneumatocysts and stipes (Max average DIC concentrations 1,813 µM ± 206

and 1,908 ± 173 µM, respectively) (Fig. 5B-E). We calculated the precision of the methods same as we did for the DOC results. We saw smaller variations in DIC with bags containing the pneumatocysts, blades, and stipe (ranging between 1.3%-20%, 4.8%-14%, and 2.7%-9%, respectively). However, we saw the largest variations with the whole intact segment (3%-30%).

In the oxic incubations, we generally saw little change of the DIC concentrations in the bags containing pneumatocysts, blades, and whole intact segments (Fig. 5F-J). DIC concentrations in the bags containing stipes had on average more DIC after approximately 400 hours (Max average DIC concentrations 2,627 µM ± 1,822 µM). Compared to the anoxic incubations the precision of the methods for DIC concentrations across our technical replicates of each component were found to be much lower and below the target 10% threshold of our SOPO ranging between 0.13% to 8.16%. However, precision in the bags containing blades and whole intact segments at the 400-hour timepoint did exceed the 10% threshold at 21% and 48%, respectively.

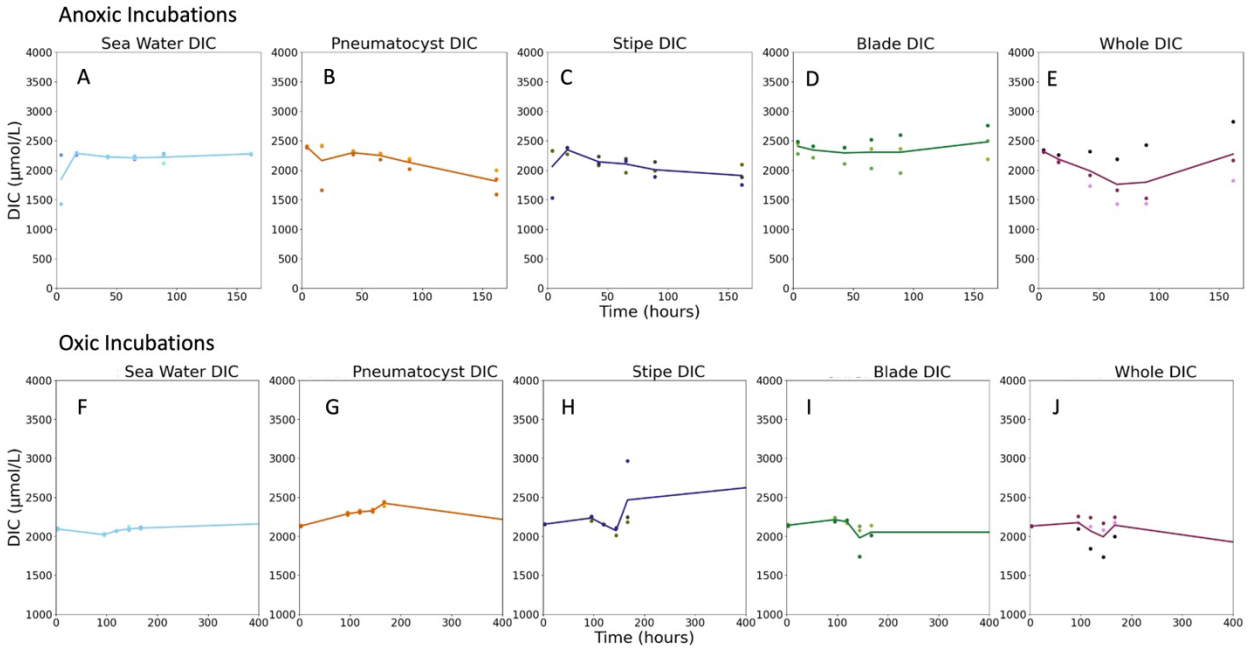

Figure 5. Results showing the evolution of DIC concentrations in bags containing Giant Kelp components during the anoxic (A-E) and oxic (F-J) kelp degradation incubations. Note the differences in the incubation time scale on the x-axis.

It is interesting that although we do see buildup of DOC and POC, particularly in the bags containing blades and whole intact segments, the DIC patterns either decreased or stayed flat. We have not pinpointed the exact mechanism that explains these patterns. However, it is possible that some of the inorganic carbon is locked up in the solid phase (i.e., carbonates) which was not determined in our experiments. Another possible explanation is that the kelp were performing dark carbon fixation which Giant Kelp are known to exhibit according to (Kremer, 1979). Alternatively, since our incubations are a closed system with a finite amount of available oxygen the incubation may not generate a large DIC buildup during our incubations. Moving forward with future experiments, we want to include longer incubations and replenish oxygen

periodically that may provide us with more information about the dynamics behind DIC production from degrading kelp biomass.

Field-based kelp decomposition experiments

In late Summer and early Fall, 2023 we saw a rebound of the local kelp forests that provided an opportunity to deploy kelp biomass packed in packages (i.e., slinky pots and burlap sandbags) to the seafloor and measure kelp degradation in the field. To do so we attached kelp packages to moorings in approximately 100 meters of water in two different locations off the coast of Santa Barbara, Ca. Two pairs of moorings were deployed in September and again in November of 2023.

In both attempts, we were successful at deploying the moorings with kelp packages attached. Unfortunately, both pairs of moorings along with the attached kelp packages were lost. One mooring that was deployed in September was lost in part due to the method of letting the kelp packages slide down the mooring line rather than attaching them to the end of the mooring line prior to deployment. The surface buoy of the mooring did not have enough lift to keep the mooring vertical resulting in the entire mooring to sink. We believe the sunken mooring is still on the seafloor at the location we placed it and have made several attempts to trawl the area with a grapple to recover the sunk mooring; however, these operations thus far have been unsuccessful. The other mooring that was deployed in September that did not sink had its surface buoy severed from the mooring after several weeks. The buoys were found washed up on a beach ~25 miles east of the original mooring location. We suspect a ship or a boat struck the surface buoys which resulted in the loss of the mooring. Afterwards we assembled 2 new moorings, this time with larger surface buoys with better lift and visibility and also a 10 ft bike lock cable made with steel leading up to the surface buoy to reduce the chance of damage from ship or boat strikes. These two new moorings were successfully deployed with kelp packages in a new location where we predict there will be less ship and boat traffic. Four weeks after the deployment, we checked on the moorings and planned to collect data; however, both moorings could not be located. It is unclear what happened to the moorings, as there was no evidence of the moorings at the site locations, but theft or accidental ship strike are not out of the range of possibilities.

Moving forward we are currently obtaining materials and constructing new moorings. The new moorings will be similar to the moorings deployed in November; however, we plan to add subsurface buoys with galvanic release and/or timer-release systems in the event the surface buoy is detached from the rest of the mooring. We also plan to purchase buoys that are equipped with GPS trackers to monitor the location of the moorings in real time. In addition, we have ordered acoustic release systems that will allow us to deploy packages in deeper water with a higher chance of recovery of kelp packages from the seafloor. Lastly, we plan to deploy the new moorings further east in deeper water and with less ship and boat traffic to minimize ship strike potential. We are optimistic that our new designs and mooring locations will lead to successful

deployment and recovery of kelp packages to determine the fate of kelp biomass in the environment, but these issues have in the meantime delayed this deliverable.

Kelp raft experiments in the UCSB Lagoon

While we were preparing new moorings for field-based kelp degradation experiments, we have set up an experiment to investigate the age of floating kelp and determine the time it takes for kelp to start sinking. We are currently conducting this experiment in the UCSB lagoon (Fig. 6). The lagoon is a low energy environment compared to the open ocean and also is easily accessible for investigators to do experiments. The lagoon has similar salinities to seawater as it constantly fed with ocean seawater. We have tethered a total of 10 fronds of varying length (max length ~ 10 meters) on a line within the lagoon (Fig 6A and B.). We will be measuring the total frond length and blade lengths to get a better understanding of kelp raft age and also note when the fronds are no longer floating at the surface (Fig. 6C). These experiments are ongoing and we expect to have data to show in the QR meeting in March.

Figure 6. Picture of the UCSB lagoon (A) with floating kelp fronds (B) and measuring kelp frond and blade length (C).

Task 4 – Modeling the environmental impacts of seaweed cultivation and sequestration

Deliverable – None

Leads: Daniel Dauhajre, Danielle Bianchi, Ahn Pham & Jim McWilliams (all UCLA) & David Siegel (UCSB)

We continue the model development targeting a virtual seaweed mCDR experiment in the Southern California Bight (Task 4.5-4.6) with an initial deployment of ROMS-BEC-MAG in an

idealized channel configuration. This idealization allows us to systematically develop and implement model components (Task 4.4, 100% complete) to simulate giant kelp cultivation, its interaction with circulation and biogeochemistry, and vertical conveyance of biomass in a controlled environment. The primary development this quarter is the design and implementation of reactive vertical conveyance of kelp biomass in ROMS-BEC (see Figs. 7 and 8). Additionally, we are continuing our validation and tuning of the streamlined macroalgal growth model (MAG) (Task 4.3, 100% complete). For the latter, we are testing parameterizations of frond senescence to include this effect in the mortality rate. The development and implementation of the ROMS-BEC-MAG CDR modeling system (Task 4.4) is provisionally written up in a technical document. This document will constitute the methods section for a peer-reviewed journal article in preparation. This journal article will describe the fully coupled CDR modeling system and demonstrate model functionality and farm-environment interactions with a set of idealized experiments. These idealized experiments will be presented at OSM 2024 (session CM004), with an initial set of experiments briefly described below.

We have conducted a set of four seaweed CDR experiments in the idealized channel configuration (Fig. 7). This configuration is the same as reported in QR4-5 and is a computationally efficient test-bed for experimentation and model refinement. For each experiment, we prescribe a surface flux (or 'injection') of a kelp biomass specific tracer (C_kelp [mmol C / m^3]); the surface flux in all four experiments is equivalent to 1 kg C / m^2 / month and injected over a farmed area of 3 km x 1.8 km. For two cases, this surface injection is constant in time (green and black curves, Fig. 7). For the other two cases (blue and red cases, Fig. 7), this surface injection is prescribed as a periodic impulse function (15 days of injection followed by15 days of no injection); the latter is meant to demonstrate the capacity to simulate time (or space) variable harvest and sinking strategies. We prescribe a sinking rate of 0.01 m/s (informed by experiments in Task 2) in three of the cases (black, green, and blue curves in Fig. 1). To test the sensitivity to sinking rate, we run one case with a 0.001 m/s sinking rate(red curve, Fig. 7); unsurprisingly, this case results in a slower rate of bottom accumulation of carbon.

Fig. 7 and 8 demonstrate the accumulation of kelp carbon in the near-bottom (Fig. 7) and water-column (Fig. 8) in these experiments as well as the production of DOC and DIC that result from the remineralization of C_kelp. This remineralization and DOC and DIC production behaves as a function of ambient temperature and oxygen and we have provisionally assumed an equal partition of DIC and DOC production from the remineralization of C_kelp. The general agreement between the green and black curves in Fig. 7 indicates that the surface wind stress and boundary layer mixing do not appreciably impact the biomass accumulation, primarily due to the rapid sinking rate; the upper-ocean biogeochemical cycling and flow-farm interaction are marginally modified by the wind forcing (not shown); we expect these differences to increase with wind speed. Fig. 8 shows a cross-section snapshot (at t=25 days) of the kelp carbon tracer and DOC anomaly (defined relative to a horizontal average) for the constant sinking and wind-

forced case (green curve, Fig. 7). Note the positive DOC anomaly associated with the sinking kelp biomass that is also carried downstream by the inflow (that flows from left to right and extends down to 300 m).

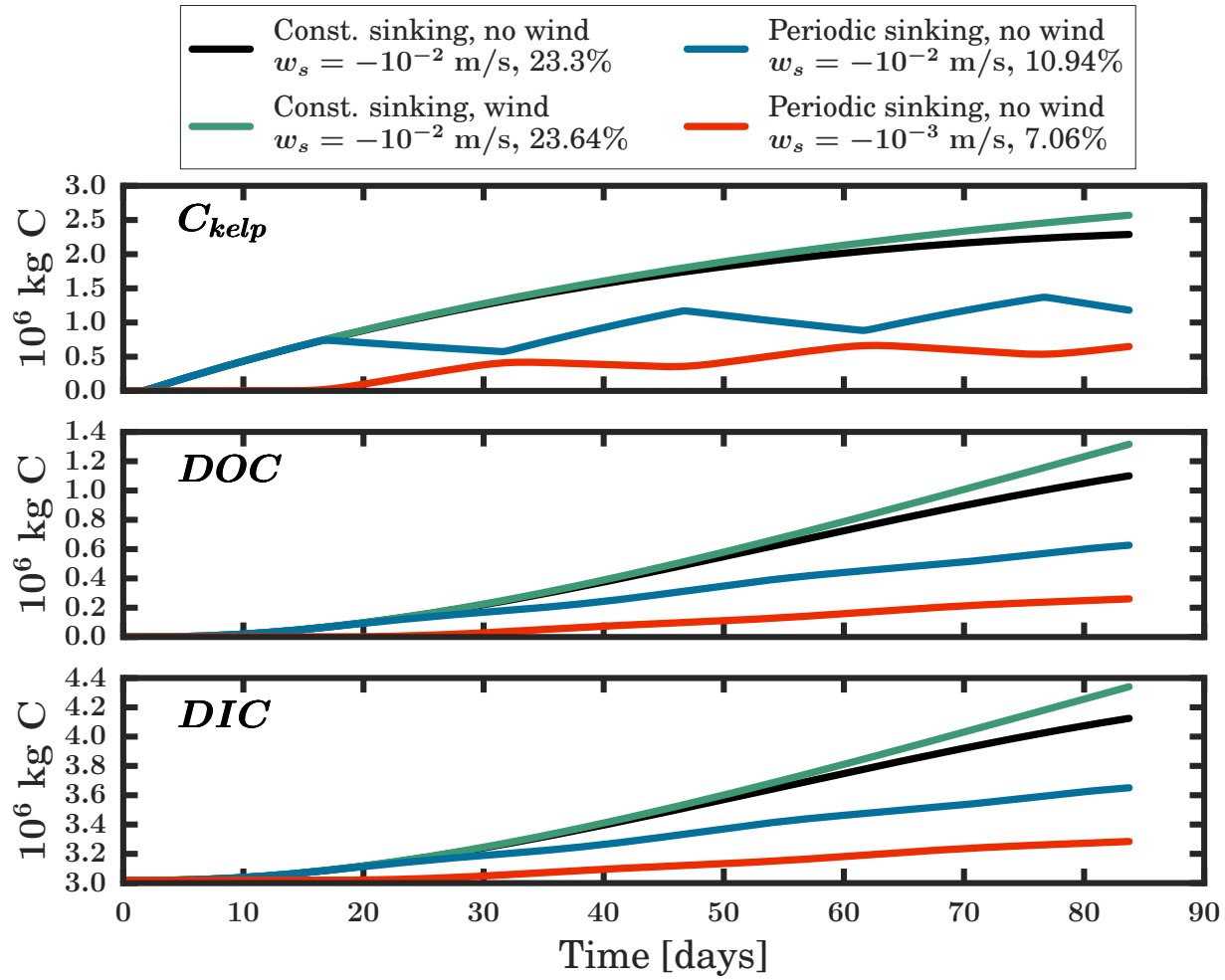

Fig. 7: Time-series of volume-integrated, near-bottom kelp biomass (top), DOC (middle), and DIC (bottom) for four idealized experiments (colors). The volume integral is taken over a horizontal area of approximately 16 km^2 (surrounding the farm footprint) and from the seafloor up to 10 m above the bottom. The legend indicates each experiment (described in the text) and the sinking velocity (w_s). The percent value indicated for each case is the percentage of C_kelp that accumulates near the bottom after 1 month, relative to the surface injection. Note the DOC and DIC production, indicating the remineralization of C_kelp, as well as the influence of w_s (red versus blue) on bottom accumulation rate.

The aim of ongoing and future work is to continue testing the vertical conveyance implementation and coordinate parameter sensitivity tests (sinking rate, remineralization parameters) with experimental results obtained in Tasks 2 and 3. Given the relatively fast sinking rates observed in Task 2, the biomass reaches the seafloor (~1500 m depth) very quickly (~1-2 days for w_s =-0.01 m/s). This motivates future, careful consideration of treatment for benthic decomposition of kelp biomass in the model as well as future exploration of near-bottom currents

in the Southern California realistic configuration. These non-steady currents will likely impact the fate and transport of DOC and DIC plumes generated at sinking sites.

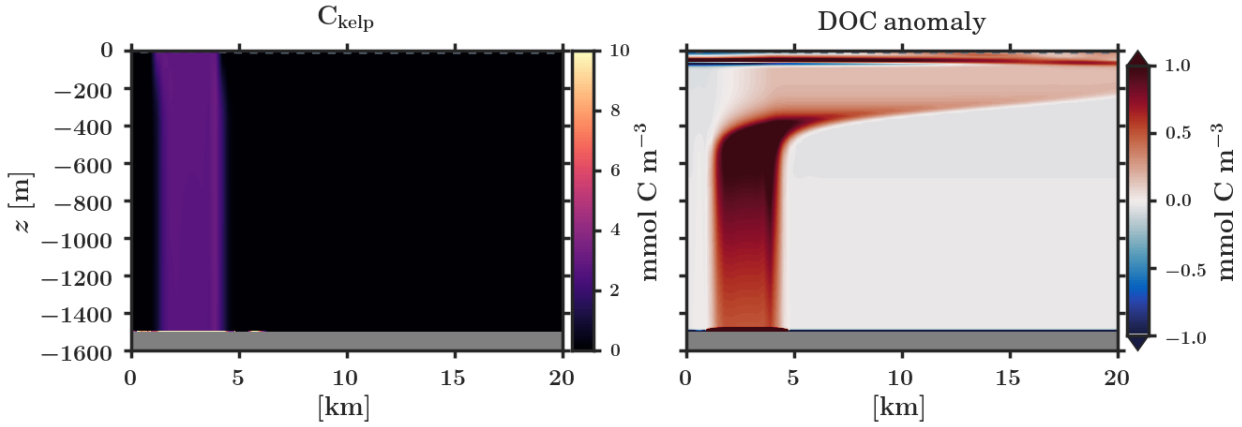

Fig 8: Cross-section (across-farm axis, depth) snapshot (t=25 days) of the reactive kelp carbon tracer (C_kelp, left) and the DOC anomaly (right) in an idealized CDR experiment. This snapshot corresponds to the green curve experiment in Fig. 1. The DOC anomaly is defined relative to the horizontal mean at every depth. Note the accumulation of C_kelp in the bottom, that is continually fed by the surface production (1 kg-dry / m^2 / month) and sinking rate of 0.01 m/s. As the kelp sinks, it remineralizes and produces DOC (right); some of this DOC is transported horizontally before reaching the bottom by the near-surface current. The colorbars are saturated (particularly relative to bottom values) to allow clearer visualization of mid water- column concentrations.

Task 6 – Technology to Market

Deliverable – M6.3 - Establish Stakeholder Advisory Board - completion = 100%

First draft of the T2M has been submitted to ARPA-E for iteration

M6.7 - Scientific Outreach - completion = 15%

One peer reviewed paper has been published this reporting period (Nowicki et al. 2024). This paper addresses organic carbon storage by the natural biological pump and the very significant role of finite time of air-sea CO_2 exchange (increases carbon storage by ~35% globally). Of importance to this project, we developed and validated a linearized modeling framework for this problem that can also be easily applied for assessing the time scales of sequestration for any mCDR approach including finite time gas transfer. The application of this modeling framework for understanding the time scales of mCDR sequestration will be presented in two presentations at the upcoming Ocean Sciences Meeting (Sten et al. and Yamamoto et al.).

To date, we have published on the preprint server EarthArXiv three white papers detailing rationale and procedures for several aspects of the SeaweedCDR project. These white papers

have Digital Object Identifiers (DOIs) and hence are searchable in Google Scholar and other tools. We consider these publications as appendices for scientific publications that will follow once we have completed our research objectives. The four white papers published to date are listed below. As mentioned previously, a fifth white paper on modeling the impacts of seaweed cultivation and sequestration biomass is undergoing internal review and will be submitted to EarthArXiv preprint server shortly.

It should also be mentioned that five participants from the SeaweedCDR project have submitted 5 abstracts to the 2024 Ocean Sciences Meeting in New Orleans, LA. These presentations will be Authors and abstract titles are listed below.

References:

English, C. J. and Carlson, C. A.: Protocols for the quantification and characterization of dissolved organic carbon from seaweed and its sequestration potential, 2023.

Krause, S. J. E., Matsumura, S., English, C. J., Carlson, C. A., Miller, R., Valentine, D., and Siegel, D.: Methods for assessing Giant Kelp (Macrocystis pyrifera) biomass sinking rates and decomposition for carbon dioxide removal applications, 2023.

Kremer, B. P.: Light independent carbon fixation by marine macroalgae 1, Journal of Phycology, 15, 244-247, 1979.

Reed, D. C., Carlson, C. A., Halewood, E. R., Nelson, J. C., Harrer, S. L., Rassweiler, A., and Miller, R. J.: Patterns and controls of reef-scale production of dissolved organic carbon by giant kelp M acrocystis pyrifera, Limnology and Oceanography, 60, 1996-2008, 2015.

Wernberg, T. and Filbee-Dexter, K.: Grazers extend blue carbon transfer by slowing sinking speeds of kelp detritus, Scientific Reports, 8, 17180, 2018.

SeaweedCDR Publications to Date:

Project Peer Reviewed Journal Articles to Date:

Nowicki, M., DeVries, T., & Siegel, D. A. (2024). The influence of air-sea CO_2 disequilibrium on carbon sequestration by the ocean's biological pump. *Global Biogeochemical Cycles*, *38*, e2023GB007880. https://doi. org/10.1029/2023GB007880.

Project White Papers Published This Quarter:

Krause, S., Matsumura, S., English, C., Carlson, C., Miller, R., Valentine, D., Siegel, D., 2023, Methods for assessing Giant Kelp (*Macrocystis pyrifera*) biomass sinking rates and decomposition for carbon dioxide removal applications, Eartharxiv, https://doi.org/10.31223/X5FH6W

Project White Papers Published Previous Quarters:

Dauhajre, D.P., Bell, T. and Siegel, D., 2023. Considerations for Regional Simulations of Seaweed Carbon Dioxide Removal. White paper available at https://doi.org/10.31223/X52Q1N.

Krause, S.J.E., Dauhajre, D.P., Bell, T., Miller, R., Valentine, D. and Siegel, D., 2023. Comparing kelp conveyance strategies for marine carbon dioxide removal with farmed macroalgae. White paper available at https://doi.org/10.31223/X5M66B.

English, C.J. and Carlson, C.A., 2023. Protocols for the quantification and characterization of dissolved organic carbon from seaweed and its sequestration potential. White paper available at https://doi.org/10.31223/X5167F.

Project Presentations for this Quarter:

Dauhajre, D., D. Bianchi, A. Pham, J.C. McWilliams, C. Frieder, T.W. Bell, S. Krause, C. English, N. Eegholm, K.A. Davis, C.A. Carlson, D.L. Valentine, R.J. Miller and D. Siegel, 2024, Towards a regional, coupled modeling system to robustly quantify the viability and environmental impacts of seaweed mCDR. Presentation to be made at the 2024 Ocean Sciences Meeting in New Orleans, LA, February 2024.

English C., and C.A. Carlson, 2024, Controls on the production and composition of macroalgal DOC and its potential contribution to coastal ocean carbon budgets. Presentation to be made at the 2024 Ocean Sciences Meeting in New Orleans, LA, February 2024.

Krause, S., S. Matsumura, D. Dauhajre, R.J. Miller, D.L. Valentine and D. Siegel, 2024, Comparing conveyance strategies and determining the fate of Giant Kelp (*Macrocystis pyrifera*) biomass for marine carbon dioxide removal. Presentation to be made at the 2024 Ocean Sciences Meeting in New Orleans, LA, February 2024.

Sten, M., Yamamoto, K., T. DeVries and D.A. Siegel, 2024, Large-scale seaweed cultivation and its purposeful sequestration: influence of vertical conveyance methods on durability. Presentation to be made at the 2024 Ocean Sciences Meeting in New Orleans, LA, February 2024.

Yamamoto, K., T. DeVries and D.A. Siegel, 2024, The importance of using an interactive ocean-atmosphere model in estimating the durability of marine-based CO_2 removal methods. Presentation to be made at the 2024 Ocean Sciences Meeting in New Orleans, LA, February 2024.

Project Presentations in Previous Quarters:

Siegel, D.A., 2023, Quantifying the efficacy & environmental impacts of large scale macroalgal cultivation & purposeful carbon sequestration. Invited oral presentation made at the Seagriculture USA 2023 in Portland ME on September 7, 2023.